

# c(2x2) Interface Alloys in Co/Cu Multilayers - Influence on Interlayer Exchange Coupling and GMR

P. Zahn and I. Mertig

Institut für Theoretische Physik

Technische Universität Dresden, D-01062 Dresden, Germany

November 9, 2018

## Abstract

The influence of a c(2x2) ordered interface alloy of 3d transition metals at the ferromagnet/nonmagnet interface on interlayer exchange coupling (IXC), the formation of quantum well states (QWS) and the phenomenon of Giant MagnetoResistance is investigated. We obtained a strong dependence of IXC on interface alloy formation. The GMR ratio is also strongly influenced. We found that Fe, Ni and Cu alloys at the interface enhance the GMR ratio for in-plane geometry by nearly a factor of 2.

## 1 Introduction

In the context of magnetoelectronic applications structural properties of the interfaces in nanostructured devices have attracted huge attention. Especially, the properties of the ferromagnet/nonmagnet (FM/NM) interface are expected to be crucial for new phenomena like oscillatory IXC and GMR that occur in magnetic layered systems. Several experiments have shown that even in the best homoepitaxially grown samples interdiffusion at the interfaces exists. The formation of, even partially ordered surface alloys on a Cu(001) substrate was reported for, e.g. Mn [1], Fe [2, 3] and Co [4]. Recent experiments on Co/Cu spin valve systems have shown the high sensitivity of the magnetotransport on the interface properties by introducing 3d scattering centers at various positions in the Co and Cu layer ( $\delta$ -layer doping) [5]. The Co/Cu(001) system is a model system for magnetism in systems with reduced dimension [6]. The lattice mismatch is rather small (about 2%) and the materials are completely immiscible in the bulk phase. Our investigations are focussed on the electronic properties of ordered interface alloys in a Co/Cu(001) multilayer system. The formation of QWS arises from the confinement of the Cu electrons. The strong correlation between IXC and quantum well states will be demonstrated. The influence on magnetotransport properties will be discussed.

## 2 Method

The electronic structure of the considered systems was calculated selfconsistently using a Screened Korringa-Kohn-Rostoker (KKR) method [7, 8, 9] based on a Green's function multiple scattering formalism. The screening procedure is an exact reformulation of the traditional KKR method [10, 11] to accelerate and simplify the numerical solution of the Dyson equation for the Green's function. The numerical effort scales linearly with the size of the unit cell for systems with a prolonged supercell. The systems were modelled as superlattices with a complex unit cell periodically repeated in 3 dimensions. That means, we consider infinite multilayer structures and exclude the influence of surfaces. The Co layer thickness was fixed to 9 monolayers (ML),  $\approx 1.6nm$  following the experimentally investigated systems. We neglect all lattice relaxations at the interfaces. All atomic positions are fixed to an ideal fcc lattice with a lattice constant of  $6.76 a.u.$ . The chosen lattice constant lies between the bulk lattice constant of magnetic fcc Co ( $6.7 a.u.$ ) and fcc Cu ( $6.83 a.u.$ ). We use spherical potentials in the atomic sphere approximation (ASA). The exchange and correlation part is described by means of the local spin density approximation in the parametrization of Vosko, Wilk and Nusair [12]. The angular momentum expansion of the Green's function was treated up to  $l_{max} = 3$  and for the charge density up to  $l_{max} = 6$ . To simulate the  $c(2 \times 2)$  ordered interface alloy we replace every second atom in the Co interface layer by a 3d element (V, Cr, Mn, Fe, Co, Ni, and Cu, resp.), which causes an increase of the in-plane unit cell by a factor of 2.

## 3 Stability of ordered Interface Alloy

It was shown by several authors [13, 14, 15, 16, 17] that the structural properties of the interfaces play an important role for the interlayer exchange coupling and GMR. The amplitude of IXC and the GMR ratio can change drastically. We demonstrate that the structural properties of the interfaces are crucial for magnetotransport properties in multilayer systems. The interface structure depends strongly on growth conditions during the preparation process. Besides mesoscopic roughness and interdiffusion the formation of an ordered interface alloy may occur. The paper is focussed on the role of ordered interface alloys. First of all we will discuss the stability of the interface alloys in a Co/Cu multilayer. For this purpose we compare the total energy of three different interface configurations: 0) the ideal atomically flat interface with  $c(1 \times 1)$  symmetry, 1) one intermixed interface layer with the same number of Co and Cu atoms equally distributed with  $c(2 \times 2)$  symmetry, and 2) two intermixed interface layers with  $c(2 \times 2)$  symmetry. The considered superlattice of type 0 consist of 9 ML Co and 7 ML Cu. For type 1 and 2 the number of Co layers is reduced by the intermixed layers to keep the Cu thickness constant. The interface formation energy is defined to be

$$E^f = E^I - n_{Co}E_{Co} - n_{Cu}E_{Cu} \quad (1)$$

where  $E^I$  denotes the total energy of the superlattice with one of the above described interface configurations.  $E^I$  is compared with the total energies of the bulk systems Co

and Cu, respectively. The bulk calculations have been performed at the same lattice constant used in the supercell calculation.  $n_{Co}$  and  $n_{Cu}$  are the numbers of *Co* and *Cu* atoms in the unit cell, respectively.  $E^f$  and all other energies are normalized to an interface area of the c(1x1) structure. We obtain the following values:  $E_0^f = 190meV$  for the ideal interfaces,  $E_1^f = 240meV$  for one intermixed atomic layer and  $E_2^f = 410meV$  for two intermixed interface layers. The energetical most favourable configuration is the ideal Co/Cu interface. This result is in line with the immiscibility of the materials at low temperatures. The energy difference of  $50meV$  between the ideal and the one intermixed layer configuration is of the order of the total energy difference resolution of our method. Kinetic reasons during the growth process can stabilize the configuration with one intermixed layer. The formation energy of the interface with 2 intermixed layers is remarkable larger. These results indicate that the c(2x2) structures found at surfaces with monolayer and submonolayer coverage of *Co* on *Cu*(001) [4] should remain at interfaces in multilayers, too. The magnetic interaction of the Co layers (IXC) mediated by the Cu electrons is RKKY-like and for this system about  $1meV$ . The magnetic interaction of adjacent interfaces due to the finite Co thickness is expected to be of the same order. Both contributions are negligible in comparison to the interface formation energy  $E^f$ .

## 4 Local Density of States

We discuss the spin dependent local density of states (LDOS) derived from the diagonal part of the Green's function and the obtained magnetic moments of the alloy constituents to characterize the electronic structure

$$n^\sigma(E, \mathbf{r}) = -\frac{1}{\pi} \Im G^\sigma(E, \mathbf{r}, \mathbf{r}) \quad . \quad (2)$$

We denote the alloy constituents by impurities in the sense of a periodic impurity arrangement in the interface atomic layer. Figure 1 shows the LDOS in the impurity Wigner-Seitz sphere for both spin directions. The energy is given relative to the Fermi level which is fixed by the underlying *Co/Cu* superlattice. The system with the ideal interfaces corresponds to the *Co* interface alloy and has c(1x1) symmetry. The local density of states are comparable to that obtained for 3d impurities in bulk *Co* [18]. For *V*, *Cr* and *Mn* we obtain a sharp virtual bound state above the Fermi level. The less attractive Coulomb potential for the early 3d elements cannot be counterbalanced by a larger exchange-correlation potential. For the later elements *Fe*, *Ni*, and *Cu* the exchange-correlation and Coulomb potential act in opposite directions for the majority electrons. The majority d-states remain filled and nearly unchanged and the minority states are shifted to lower energies and cause a reduced magnetic moment. This behaviour reflects the differences of the impurity potentials with respect to the Co potential at the ideal *Co/Cu*(001) interface. The nearly unchanged majority spin potential along with the drastic changes in the minority channel have a strong impact on the magnetotransport properties. This will be discussed later in detail.

The magnetic moments of the impurities are shown in Fig. 2. For the early 3d impurities *V*, *Cr*, and *Mn* our calculation yields the antiferromagnetic alignment of the

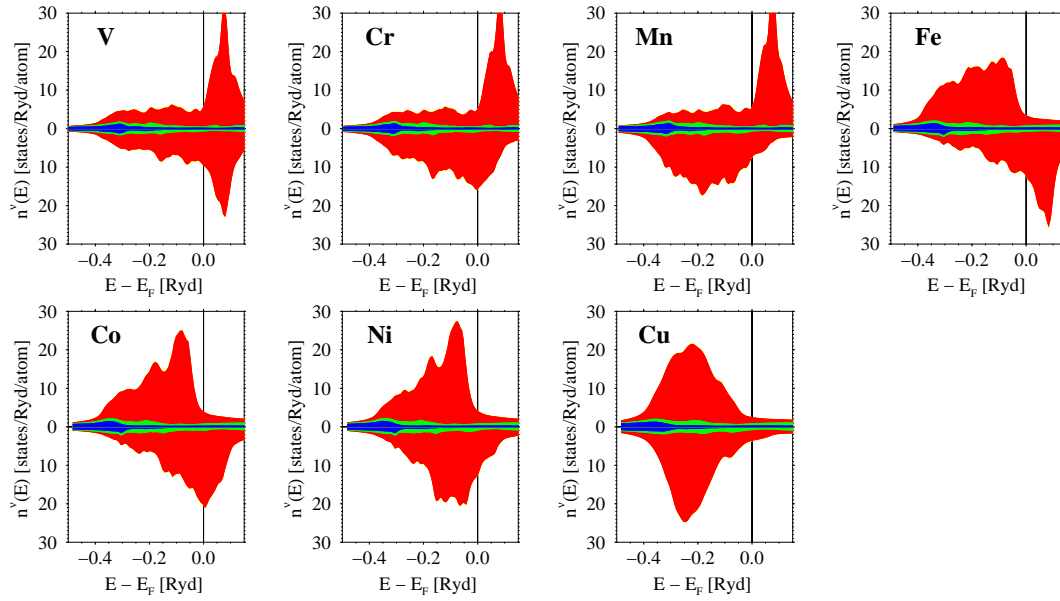


Figure 1: Local DOS of the 3d constituents of an ordered  $c(2 \times 2)$  interface alloy Co(3d) at the Co/Cu(001) interface; the blue, green and red areas correspond to partial s, p and d contributions

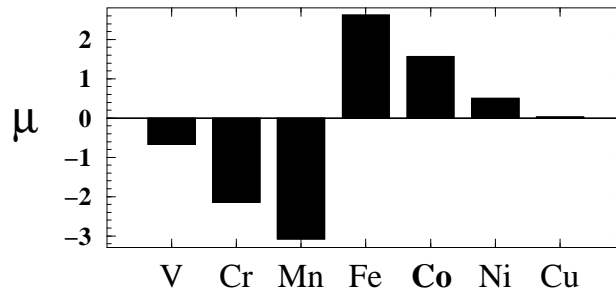


Figure 2: Magnetic moments of the 3d constituents of an ordered  $c(2 \times 2)$  interface alloy Co(3d) at the Co/Cu(001) interface

impurity moment relative to the Co moment as ground state. For the second half of the 3d series *Fe*, *Ni* and *Cu* the ferromagnetic state is energetically preferred. The size of the local moment nearly follows Hund's rule with a maximum at half d-band filling.

## 5 Interlayer Exchange Coupling

For the calculation of the strength of IXC we apply the frozen potential approximation (FPA) [19] neglecting the double counting parts in the total energy. We calculate the electronic structure for the parallel (P) alignment of the Co magnetic moments selfconsistently. The antiparallel (AP) configuration was obtained by flipping the magnetization direction in every second Co layer interchanging the fixed spin dependent ASA potentials. The strength of the IXC is then given by the single particle contributions to the total energy

$$\Delta E = E_{SP}^P - E_{SP}^{AP} \quad (3)$$

$$E_{SP} = -\frac{1}{\pi} \sum_{\sigma} \Im m \int_{-\infty}^{\mu} dE \int d^3\mathbf{r} (E - \mu) G^{\sigma}(E, \mathbf{r}, \mathbf{r}) - \mu N \quad (4)$$

with  $\mu$  denoting the chemical potential and  $N$  the total number of valence electrons. The total energy difference  $\Delta E$  is proportional to the strength of the bilinear coupling term which has a cosine dependence on the angle between adjacent Co layer magnetization directions. To determine higher order coupling terms one has to consider non-collinear magnetic configurations. Usually, the amplitudes of these contributions are much smaller than the bilinear one and consequently negligible [20].

The strength of IXC varies with the thickness  $d$  of the NM spacer layer. In the asymptotic region at large spacer thicknesses  $\Delta E$  is a superposition of oscillatory contributions. The oscillation periods are determined by stationary points of the spacer Fermi surface [13, 21]. For a *Cu* spacer in (001)-orientation 2 wellknown contributions exist, a short period from the neck region and a long period from the belly region of the 'dogs bone' orbit.

In systems with a periodic c(2x2) superstructure the in-plane real space periodicity is increased. The Fermi surface of Cu has to be folded down into a smaller Brillouin zone. This is equivalent to the occurrence of Umklapp processes due to different symmetries of spacer and FM layer. As it was shown by Kudrnovský et al. a new stationary point on the Cu Fermi surface appears [22]. The corresponding period is very short ( $\approx 2.15ML$ ). All stationary points and periods obtained in our calculation are summarized in Tab. 1. The different oscillatory contributions to the IXC energy are characterized by their amplitudes  $A_i$  and phases  $\phi_i$

$$\Delta E = \sum_{i=1}^3 \frac{A_i}{d^2} \sin\left(\frac{2\pi}{\lambda_i}d + \phi_i\right) \quad . \quad (5)$$

These parameters are determined by the coupling of the Cu electrons to the polarized electrons in the Co layers. They are influenced by the thickness and chemical composition of the FM layer and the interface structure. The decay with the square of the spacer

Table 1: Stationary points of  $Cu$  in (001) orientation with a  $c(2 \times 2)$  in-plane superstructure and corresponding oscillation periods of IXC

	$\mathbf{k}_i^{\parallel} [\frac{\pi}{a}]$	$\lambda_i [ML]$
$\mathbf{k}_1$	(0, 0)	5.89
$\mathbf{k}_2$	( $\pm 0.785, \pm 0.785$ )	2.61
$\mathbf{k}_3$	( $\pm 1, 0$ ), ( $0, \pm 1$ )	2.15

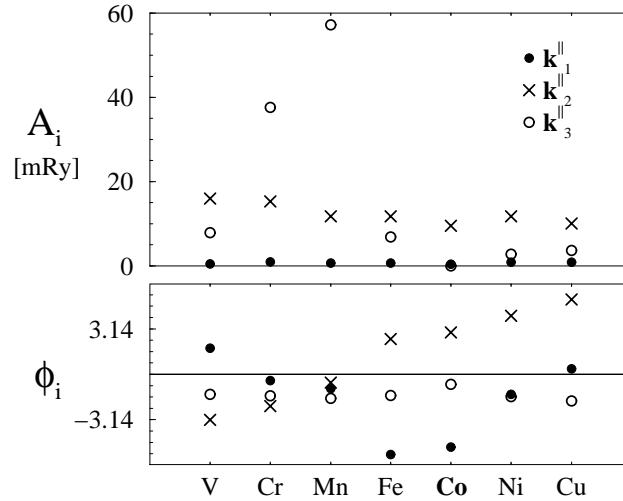


Figure 3: Amplitudes  $A_i$  and phases  $\phi_i$  of the oscillatory contributions to IXC (Eq. 5) in dependence on constituents for ordered  $c(2 \times 2)$  alloys at the Co/Cu interface

thickness arises from the screening of a 2-dimensional perturbation in a noninteracting electron gas. To determine the oscillatory contributions of IXC we calculated the coupling strength in dependence on the Cu spacer thickness. The Co layer thickness was fixed and both interfaces of the Co layers were decorated with an ordered  $c(2 \times 2)$  alloy of the 3d elements. The Cu thickness was varied in integer steps between 7 and 60 ML. Calculating the single-particle contribution of the total energy the density of states is obtained from the diagonal part of the Green's function by a Brillouin zone integration. To accelerate this integration a Fermi-Dirac occupation function for the single-particle states with a finite temperature of 400K is used [23]. This smearing of the Fermi edge results in an exponential damping of the coupling energy for spacer thicknesses much larger than a critical value  $L$  [21]. The decay length  $L$  is about 20 ML for the used temperature, spacer material and crystal orientation.

From a discrete Fourier transformation at the known periods  $\lambda_i$  we obtain the amplitudes and phases of the different contributions. Figure 3 shows the amplitudes  $A_i$  and phases  $\phi_i$  for the three contributions. The amplitude  $A_1$  of the long period oscillation is very small for all considered systems including the ideal Co/Cu superlattice. The amplitude  $A_2$  of the short period oscillation dominates the coupling energy for nearly all systems and varies by about 30%. The largest variations were found for the amplitude

$A_3$  of the oscillation caused by the superstructure. Due to symmetry arguments the amplitude  $A_3$  vanishes for the system with ideal interfaces. This system has a  $c(1 \times 1)$  in-plane symmetry and  $\mathbf{k}_3$  is not a stationary point at the Cu Fermi surface. The amplitude  $A_3$  dominates for the systems with *Cr* and *Mn* interface alloys and is about 3 times larger than the short period amplitude  $A_2$ . To elucidate the origin of this large contribution to the interlayer coupling strength we focus on the formation of quantum well states in the multilayer structure.

## 6 Quantum Well States

The description of the IXC in the RKKY picture was successfully applied to explain the oscillatory contributions and the periods [21]. To determine the phases and amplitudes of the oscillations the resulting electronic structure of the multilayer has to be examined. Crucial for the IXC is the occurrence of spin polarized localized states (QWS) in the spacer layer near the Fermi level. The boundary conditions caused by the spin dependent potential give rise to the formation of QWS. Changing the relative orientation of the magnetization direction of adjacent Co layers the energy of the QWS is shifted. In case quantum well states are shifted across the Fermi level the redistribution of electrons causes a change in the total energy and leads to the preference of one magnetic configuration to the other.

To elucidate the drastic changes in the amplitudes of the IXC contributions in dependence on the alloy constituent we investigated the  $\mathbf{k}$ -projected partial LDOS (kpLDOS) at the Fermi level. We obtain this quantity by integrating the diagonal part of the one-electron Green's function in real space over the Wigner Seitz sphere and in reciprocal space over  $k_\perp$  perpendicular to the plane

$$n_l^\nu(\mathbf{k}_\parallel) = -\frac{1}{\pi} \sum_m \int dk_\perp \Im G_{LL}^{\nu\nu}(z, \mathbf{k}_\parallel, k_\perp) \quad . \quad (6)$$

$L = (l, m)$  is a short hand notation for orbital and magnetic quantum number,  $\nu$  is the site index in the unit cell and  $z$  the Fermi energy  $\epsilon_F$  with a small complex part  $\Gamma$  of about  $0.2eV$  to achieve a better convergence in the  $k_\perp$  integration. The kpLDOS is related to the probability amplitude of the eigenstates at the Fermi level

$$n_l^\nu(\mathbf{k}_\parallel) = \frac{1}{\pi} \sum_m \int dE \int dk_\perp \left| \Psi_{(\mathbf{k}_\parallel, k_\perp)}^{\nu L}(E) \right|^2 \frac{\Gamma}{(E - \epsilon_F)^2 + \Gamma^2} \quad (7)$$

$$\approx \sum_{k_{perp}} \delta(E - \epsilon_F) \left| \Psi_{(\mathbf{k}_\parallel, k_\perp)}^{\nu L}(\epsilon) \right|^2 \quad . \quad (8)$$

The typical probability amplitude for confined states in a layered structure can be obtained for a free electron model with potential wells in growth direction. From the boundary condition that the wave function decreases exponentially in the potential barrier one obtains an oscillatory probability amplitude inside the potential well. The oscillation period is given by the wave vector of the free states without any barrier. In the NM/FM multilayer system the potential barrier corresponds to the FM layers and the states in

the NM spacer are confined in the resulting potential. The oscillation of the probability amplitude is given by the unperturbed spacer states. A strong oscillatory variation of the probability amplitude inside the the spacer indicates a strong confinement and a large contribution to the IXC from the considered stationary  $\mathbf{k}_{\parallel}$  vector. Figure 4 shows the  $\mathbf{k}$ -projected partial LDOS at the stationary  $\mathbf{k}_{\parallel}^3$  point for the system with ideal interfaces, the *Cr*, and the *Mn* alloy. The spin-dependent kpLDOS is shown for every atomic layer for the P alignment of the *Co* magnetic moments. We remind the reader that every atomic layer is represented by 2 atoms. On the left and right are the Co layers, the dashed vertical lines mark the alloyed Co interface layers and in between is the Cu spacer. For the ideal system the states at  $\mathbf{k}_{\parallel}^3$  have a nearly constant amplitude in the Cu spacer and a strong hybridization with the Co states for both spin directions. In contrast, the minority states in the *Cr* and *Mn* alloyed systems show strong indications of quantum confinement in the spacer region. The s- and d-angular momentum contributions show clear oscillations with a period of about  $2ML$ . This coincides with the Fermi wave vector of *Cu* at  $\mathbf{k}_{\parallel}^3$  which determines the oscillation period of the superstructure contribution to IXC. At the position of the stationary point  $\mathbf{k}_{\parallel}^2$  we found for all the considered systems confined states in the *Cu* spacer for minority and majority spin electrons.

## 7 Giant MagnetoResistance

For the calculation of transport properties we use Mott's two-current model [24] neglecting spin flip scattering. For the considered systems assuming non-Kondo-impurities only this assumption should be reasonable. The linearized Boltzmann equation in relaxation time approximation was solved. One yields the spin dependent conductivity  $\sigma^{\sigma}$  from a Fermi surface integral weighted with an isotropic relaxation time neglecting the anisotropy of the scattering operator

$$\sigma^{\sigma} = \frac{e^2}{V} \tau \sum_{\mathbf{k}} \delta(\epsilon_{\mathbf{k}}^{\sigma} - \epsilon_F) \mathbf{v}_{\mathbf{k}}^{\sigma} \otimes \mathbf{v}_{\mathbf{k}}^{\sigma} \quad . \quad (9)$$

The superscript  $\sigma$  denotes the spin direction and  $V$  the crystal volume. A modified tetrahedron method was used to obtain the Fermi surface integrals [25, 26]. Assuming the same spin independent relaxation times  $\tau$  for both magnetic configurations of the Co moments (P,AP) this quantity does not enter the expression for the GMR ratio. The GMR ratio is defined in the usual way by normalizing the resistivity drop in a sufficient large magnetic field by the saturation resistivity. In terms of conductivities for the P and AP configurations this is

$$R = \frac{\sigma^P}{\sigma^{AP}} - 1 \quad . \quad (10)$$

In Fig. 5 (upper panels) the spin resolved conductivity contributions for the P configuration are shown in dependence on the interface alloy constituent. The conductivities are calculated for current in-plane (CIP) and perpendicular-to-plane (CPP) geometry. For defects with a moment parallel to the Co magnetization a large spin anisotropy occurs.



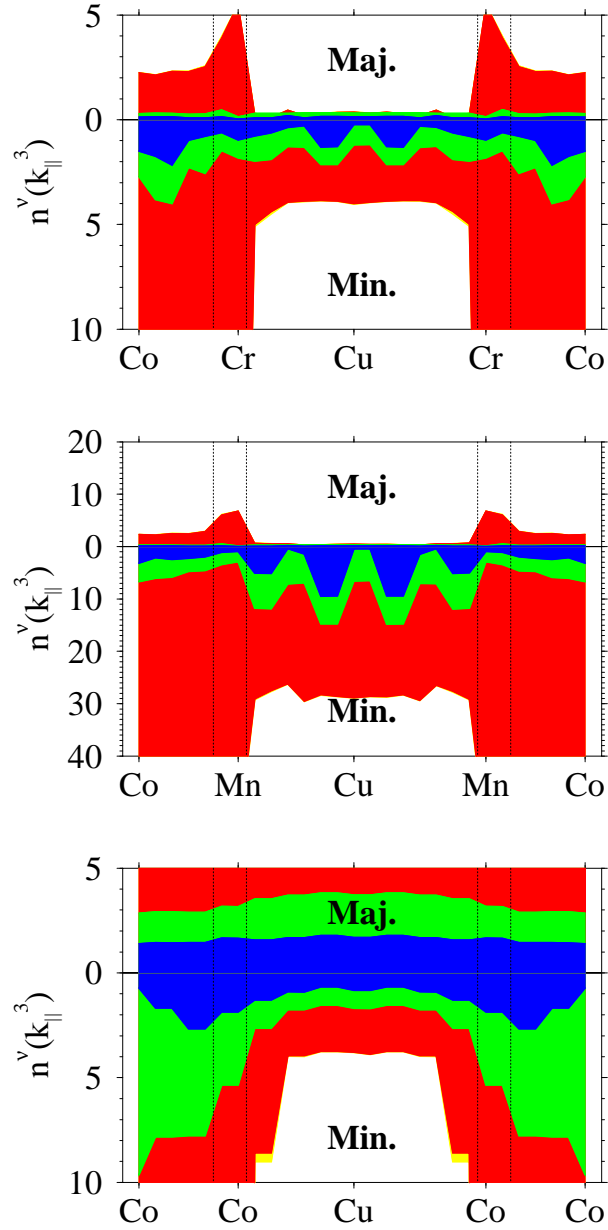


Figure 4: Spin dependent  $k$ -projected Local DOS at the stationary point  $k_{\parallel}^3$  for the *Cr* alloyed (top), the *Mn* alloyed systems (center) and the system with ideal interfaces (bottom); the blue, green and red areas correspond to partial s, p and d contributions

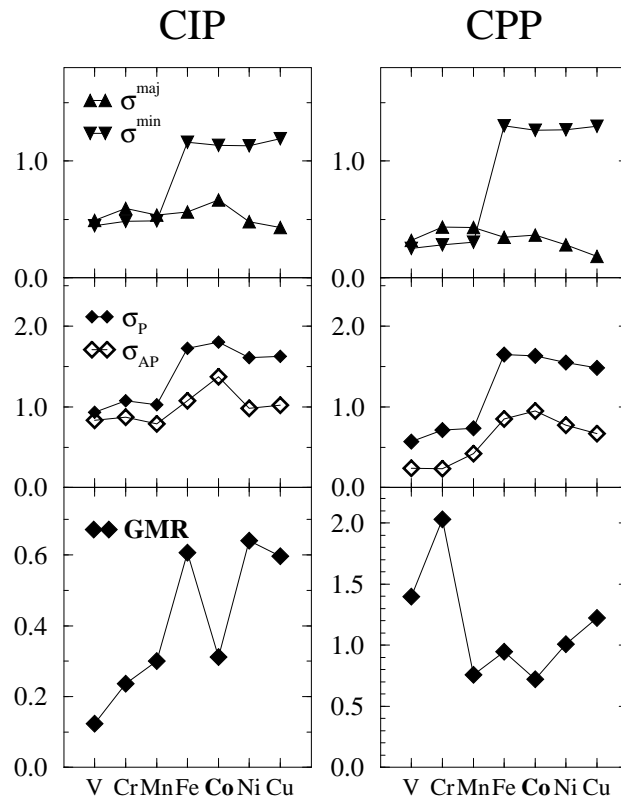


Figure 5: Spin resolved conductivities for the P configuration (top panels), conductivities for P and AP configuration (central panels) and GMR ratio (lower panels) for CIP and CPP transport in dependence on interface alloy constituent

The conductivity is dominated by the fast majority channel, especially pronounced in the CPP geometry. The occurrence of one dominating spin channel in the P configuration is essential to establish a large GMR ratio. In *Co/Cu* systems the majority potential for both materials is nearly equal whereas the minority potential has strong quantum well modulations. For the AP configuration the effective potential for both spin channels is a mixing of majority and minority potentials and causes averaged conductivities. The same effect is produced by defects with an antiparallel moment relative to the *Co* moment causing a strong perturbation of the majority potential even in the P configuration.

In Fig. 5 (central panel) the total conductivities for the P and AP configuration are compared. The relative difference determines the GMR ratio. We obtain a CIP-GMR ratio of 31% for the system with ideal interfaces. For the alloys of *Fe*, *Ni*, and *Cu* with a moment parallel to the *Co* moment the value is increased by nearly a factor of 2. In the contrary, for systems with alloys of *V*, *Cr*, and *Mn* with antiparallel moment the CIP-GMR ratio is reduced systematically. As a result, we can conclude the following empirical rule for the influence of interface alloys on CIP transport. Magnetic ordered structures with moments parallel to the ferromagnetic layers increase the GMR ratio whereas alloy constituents with antiparallel moments decrease the ratio.

In CPP geometry the GMR ratio changes by about 60% for alloys with parallel moments. In the case of antiparallel moment of the alloy constituent the spin asymmetry of the conductivity in the P configuration changes the sign and the conductivity is dominated by the minority channel. Additionally, the conductivity for AP configuration decreases rapidly for the earlier 3d elements and causes a strong enhancement of GMR for *V* and *Cr* interface alloys.

## 8 Summary

We demonstrated that the electronic structure of a *Co/Cu*(001) multilayer systems is strongly influenced by the formation of an ordered interface alloy. The correspondence between the formation of quantum well states and the strength of oscillatory IXC in dependence on the interface structure was demonstrated. We found a third oscillatory contribution to IXC arising from the *c*(2x2) interface alloy symmetry. The amplitude of this contribution varies strongly in dependence on the alloy constituent. Due to the very short oscillation period the experimental confirmation of this contribution would be a strong challenge. The GMR ratio is mainly determined by the coherent potential landscape of the multilayer. The resistivity drop is caused by the occurrence of a fast and slow channel in the P configuration. The GMR ratio decreases rapidly with the vanishing spin asymmetry of the conductivity in P configuration due to alloy constituents with an antiparallel moment.

We would like to thank G. Güntherodt, P.H. Dederichs, and J. Binder for stimulating discussions. P.Z. acknowledges the support by the German BMBF-Leitprojekt "Magnetoelektronik" (contract 13N7379).

## References

- [1] T. Flores, S. Junghans, and M. Wuttig, Surf. Sci. **371**, 1 (1997).
- [2] K.E. Johnson, D.D. Chambliss, R.J. Wilson, and S. Chiang, Surf. Sci. **313**, L811 (1994).
- [3] J. Shen, J. Giergel, A.K. Schmid, and J. Kirschner, Surf. Sci. **328**, 32 (1995).
- [4] F. Nouvertne, U. May, A. Rampe, M. Gruyters, U. Korte, R. Berndt, and G. Güntherodt, Surf. Sci. **436**, L653 (1999).
- [5] C.H. Marrows and B.J. Hickey, cond-mat/0005073
- [6] J.A.C. Bland and B. Heinrich (eds.), *Ultrathin Magnetic Structures I+II*, Springer, Berlin, (1994).
- [7] L. Szunyogh, B. Újfalussy, P. Weinberger, and J. Kollár, Phys. Rev. B **49**, 2721 (1994).
- [8] R. Zeller, P.H. Dederichs, B. Újfalussy, L. Szunyogh, and P. Weinberger, Phys. Rev. B **52**, 8807 (1995).
- [9] P. Zahn, I. Mertig, R. Zeller, and P.H. Dederichs, Phil. Mag. B **78**, 411 (1998).
- [10] J. Korringa, Physica **13**, 392 (1947).
- [11] W. Kohn and N. Rostoker, Phys. Rev. **94**, 1111 (1954).
- [12] S. H. Vosko, L. Wilk, and M. Nusair, Can. J. Phys. **58**, 1200 (1980).
- [13] P. Bruno, Phys. Rev. B **52**, 411 (1995).
- [14] J. Kudrnovský, V. Drchal, R. Coehoorn, M. Šob, and P. Weinberger, Phys. Rev. Lett. **78**, 358 (1997).
- [15] P.M. Levy, S. Maekawa, and P. Bruno, Phys. Rev. B **58**, 5588 (1998).
- [16] R. Schad, P. Belien, G. Verbanck, V. V. Moshchalkov, Y. Bruynseraede, H. E. Fischer, S. Lefebvre, and M. Bessiere, Phys. Rev. B **59**, 1242 (1999).
- [17] P. Zahn, J. Binder, I. Mertig, R. Zeller, and P.H. Dederichs, Phys. Rev. Lett. **80**, 4309 (1998).
- [18] V.S. Stepanyuk, R. Zeller, P.H. Dederichs, and I. Mertig, Phys. Rev. B **49**, 5157 (1994).
- [19] A. Oswald, R. Zeller, J. Braspenning, and P.H. Dederichs, J. Phys. F **15**, 193 (1985).
- [20] C. Blaas, P. Weinberger, L. Szunyogh, J. Kudrnovsky, V. Drchal, P.M. Levy, and C. Sommers, Eur. Phys. J. B **9**, 245 (1999).

- [21] P. Bruno and C. Chappert, Phys. Rev. Lett. **67**, 1602, 2592 (E) (1991)
- [22] J. Kudrnovský, V. Drchal, C. Blaas, I. Turek, and P. Weinberger, Phys. Rev. Lett. **76**, 3834 (1996).
- [23] K. Wildberger, P. Lang, R. Zeller, and P.H. Dederichs, Phys. Rev. B **52**, 11502 (1995).
- [24] N.C. Mott, Adv. Phys. **13**, 325 (1964)
- [25] G. Lehmann and M. Taut, Phys. Stat. solid (b) **54**, 469 (1972).
- [26] P. Zahn, PhD Thesis, TU Dresden (1998),  
<http://www.phy.tu-dresden.de/physik/publik/habildiss.htm> .